



Brain circuits signaling the absence of emotion in body language

Arseny A. Sokolov^{a,b,c,d,1}, Peter Zeidman^b, Michael Erb^e, Frank E. Pollick^f, Andreas J. Fallgatter^{g,h}, Philippe Ryvlin^a, Karl J. Friston^b, and Marina A. Pavlova^g

^aNeuroscape@NeuroTech Platform and Service de Neurologie, Département des Neurosciences Cliniques, Centre Hospitalier Universitaire Vaudois, 1011 Lausanne, Switzerland; ^bWellcome Centre for Human Neuroimaging, Institute of Neurology, University College London, WC1N 3BG London, United Kingdom; ^cNeuroscape Center, Department of Neurology, University of California, San Francisco, CA 94158; ^dDepartment of Neurology, University Neurorehabilitation, University Hospital Inselspital, University of Bern, 3010 Bern, Switzerland; ^eDepartment of Biomedical Magnetic Resonance, University of Tübingen Medical School, 72076 Tübingen, Germany; ^fDepartment of Psychology, Glasgow University, G12 8QQ Glasgow, United Kingdom; ^gDepartment of Psychiatry and Psychotherapy, University of Tübingen Medical School, 72076 Tübingen, Germany and ^hGerman Center for Neurodegenerative Diseases (DZNE), 72076 Tübingen, Germany

Edited by Peter L. Strick, University of Pittsburgh, Pittsburgh, PA, and approved July 6, 2020 (received for review April 23, 2020)

Adaptive social behavior and mental well-being depend on not only recognizing emotional expressions but also, inferring the absence of emotion. While the neurobiology underwriting the perception of emotions is well studied, the mechanisms for detecting a lack of emotional content in social signals remain largely unknown. Here, using cutting-edge analyses of effective brain connectivity, we uncover the brain networks differentiating neutral and emotional body language. The data indicate greater activation of the right amygdala and midline cerebellar vermis to nonemotional as opposed to emotional body language. Most important, the effective connectivity between the amygdala and insula predicts people's ability to recognize the absence of emotion. These conclusions extend substantially current concepts of emotion perception by suggesting engagement of limbic effective connectivity in recognizing the lack of emotion in body language reading. Furthermore, the outcome may advance the understanding of overly emotional interpretation of social signals in depression or schizophrenia by providing the missing link between body language reading and limbic pathways. The study thus opens an avenue for multidisciplinary research on social cognition and the underlying cerebrocerebellar networks, ranging from animal models to patients with neuropsychiatric conditions.

body language | social cognition | emotion | effective connectivity

Social cognition is of crucial importance for our daily life. Bodily signals are less amenable to conscious control than facial expressions and therefore, provide unbridled information about a person's intentions and affective states (1, 2). Nevertheless, research on social cognition has mainly focused on facial cues. Furthermore, most neuroimaging studies have assessed responses to affective relative to nonemotional stimuli, leaving the brain responses to neutral social signals per se beyond attention. However, adaptive social behavior and mental well-being also require inferring the absence of emotional content. This may be of particular relevance during exceptional events such as the coronavirus disease 2019 (COVID-19) pandemic involving social distancing and isolation as well as higher levels of anxiety but also, requiring intact social communication and empathy (3–5).

This study aimed at characterizing the causal interactions (effective connectivity) within the neural network underwriting the detection of the absence of an emotional expression in body language. To this end, we used dynamic causal modelling (DCM) to analyze functional MRI (fMRI) data from typically developing participants. DCM measures of directed effective brain connectivity derived from fMRI have been previously shown to represent valuable predictive markers of behavior (6). The participants viewed point-light animations of performers knocking on an invisible door with neutral or emotional expressions (Fig. 1A and Movie S1).

Results

Behavioral and Imaging Measures: Variability in the Detection of Absent Emotion in Body Language. The accuracy for inferring the absence of emotion (hit rate for neutral knocking) was 0.7 ± 0.35 (mean \pm SD). The false alarm rate (indicating absent emotion for emotional knocking) was 0.21 ± 0.19 . An exploratory whole-brain fMRI analysis ($P < 0.05$, voxelwise familywise error [FWE] corrected) revealed activation in the right amygdala and midline cerebellar vermis when contrasting neutral vs. emotional knocking (Fig. 1B and C) and in the right insula for the reverse contrast (Fig. 1D).

Effective Connectivity Reveals a Cerebello-amygdala Circuitry. A DCM analysis assessed the modulation of effective connectivity between these regions during the processing of neutral and emotional point-light knocking. Bayesian model reduction (BMR) (7) was used to identify the optimal (i.e., optimally explaining the imaging data) connectivity at the group level. These analyses indicated negative (i.e., inhibitory) effective connections from the amygdala and cerebellar vermis to insula during the processing of neutral stimuli (Fig. 2A), whereas connectivity from the insula inhibited the amygdala and cerebellum during the reading of emotional body language (Fig. 2B).

Significance

How do we infer absence of emotion? As opposed to the brain mechanisms for recognizing emotions, this issue has remained underinvestigated. Present findings bond communication between the amygdala and insula with the ability to infer the absence of emotion in body language. Previously, both the amygdala and insula have been associated with emotion perception. The outcome of this study extends the conceptualization of these brain regions and their interplay to the processing of social signals without emotional content. This may have wide-ranging implications for better understanding neuropsychiatric conditions characterized by misinterpretation of neutral for emotional signals, such as depression or schizophrenia. The findings call for interdisciplinary research on how the brain infers the lack of emotional valence in social signals.

Author contributions: A.A.S. and M.A.P. designed research; A.A.S. and M.E. performed research; A.A.S., P.Z., F.E.P., A.J.F., P.R., and K.J.F. contributed new reagents/analytic tools; A.A.S., P.Z., M.E., K.J.F., and M.A.P. analyzed data; and A.A.S. and M.A.P. wrote the paper.

The authors declare no competing interest.

This article is a PNAS Direct Submission.

Published under the PNAS license.

¹To whom correspondence may be addressed. Email: arseny.sokolov@chuv.ch.

This article contains supporting information online at <https://www.pnas.org/lookup/suppl/doi:10.1073/pnas.2007141117/-DCSupplemental>.

First published August 6, 2020.

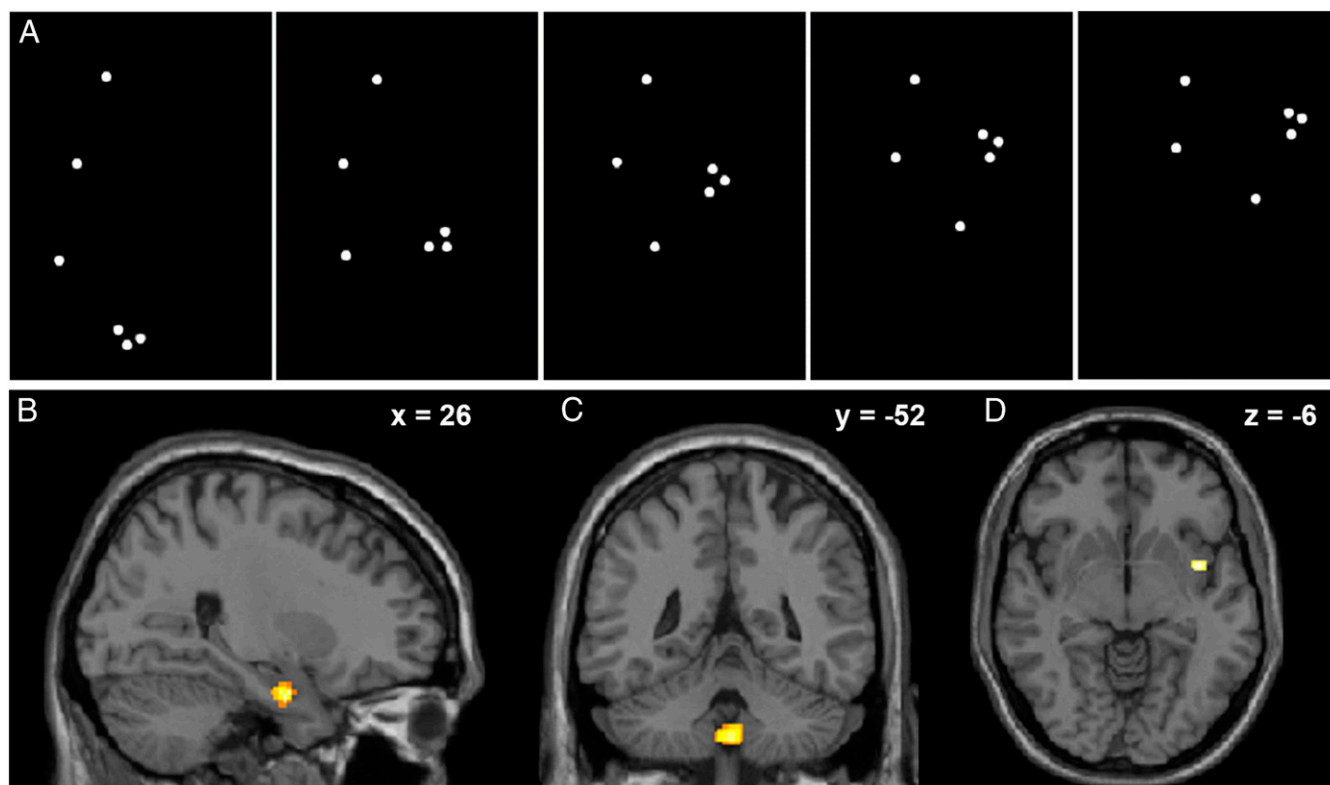


Fig. 1. Neutral and emotional point-light knocking elicited differential brain responses. (A) Five frames illustrate knocking as a set of light dots against a dark background. The dots were placed on the head, right shoulder, elbow, wrist, and first and fourth metacarpal joints of an invisible person facing to the right. (B–D) Neutral as compared with emotional point-light knocking activated (B) the right amygdala ($x = 26$; $y = 4$; $z = -26$; Montreal Neurological Institute [MNI] coordinates) and (C) midline cerebellar uvula ($x = 0$; $y = -52$; $z = -46$). (D) The right insula ($x = 44$; $y = 4$; $z = -6$) exhibited higher activation for emotional as compared with neutral knocking stimuli. Activation is overlaid on the MNI T1 template. Slice positions in MNI space are provided in the right upper corner of each panel.

The Interplay between the Amygdala and Insula Predicts Behavior.

Using estimates of connection strengths under the optimal network, we assessed subsequently whether individual variations in the effective connectivity between the insula, amygdala, and cerebellar vermis during neutral and emotional knocking were predictive of participants' behavioral inference of the absence of emotion. In participants with a hit rate to neutral knocking below 1.0, the hit rate correlated negatively with changes in connectivity from the amygdala to insula during the processing of neutral body motion (Pearson product-moment correlation, $r = -0.75$, $P = 0.01$, corrected for multiple comparisons). In other words, the greater the inhibition of the individual connections from the amygdala to insula, the better the participants identified the absence of emotion.

The modulation of the backward connection from the insula to amygdala during processing of emotional stimuli was positively correlated with the false alarm rate ($r = 0.88$, $P < 0.001$). This suggests that participants with less inhibitory effective connectivity from the insula to amygdala (i.e., disinhibition) during the processing of emotional body language had a higher propensity to label emotional stimuli as neutral. We found no significant correlation between performance and changes in effective connectivity between the insula and cerebellar uvula (Fig. 2). The processing of neutral stimuli engaged an otherwise latent, excitatory effective connection from the amygdala to cerebellar uvula. This connection was not significantly correlated with performance ($r = 0.51$, n.s.).

Discussion

Taken together, these findings indicated that modulation of the reciprocal effective connectivity between the amygdala and

insula during processing of neutral and emotional body language predicted people's ability to recognize neutral body language. The insula and amygdala are known to be strongly interconnected (8). The present study suggests that their interplay may be important not only for the processing of emotions (9, 10) but also, for inferring the absence of emotional content in body language.

At first glance, the connectivity-behavior relationships along with activation of the amygdala in response to emotionally neutral stimuli seem to contradict the considerable amount of previous data underscoring engagement of the amygdala in emotion processing (11–15). On the other hand, the brain mechanisms underwriting the discrimination between neutral and emotional body language have thus far received only little attention. Interactions between the amygdala and insula may reflect decision making during the processing of stimuli with and without emotional valence (16, 17). For instance, involvement of the amygdala has been shown in decision making, including social decisions in rats and nonhuman primates (18–20). Furthermore, intracranial recordings in patients with epilepsy implicated the amygdala in self-monitoring and processing of behavioral errors (21), a vital component of decision making and adaptive behavior. One may also interpret the present findings as an extension of the increasingly prevalent view of the amygdala as a coordinator and regulator of the networks for emotional processing (10). Parts of the amygdala may regulate emotion processing, in close interaction with the insula. According to intracranial recordings in epileptic patients, emotion processing and regulation appear to coincide in the amygdala (22). Concurrently, interdisciplinary evidence from connectivity-based parcellation (23), pharmacological studies (24), and animal research (25, 26) indicates

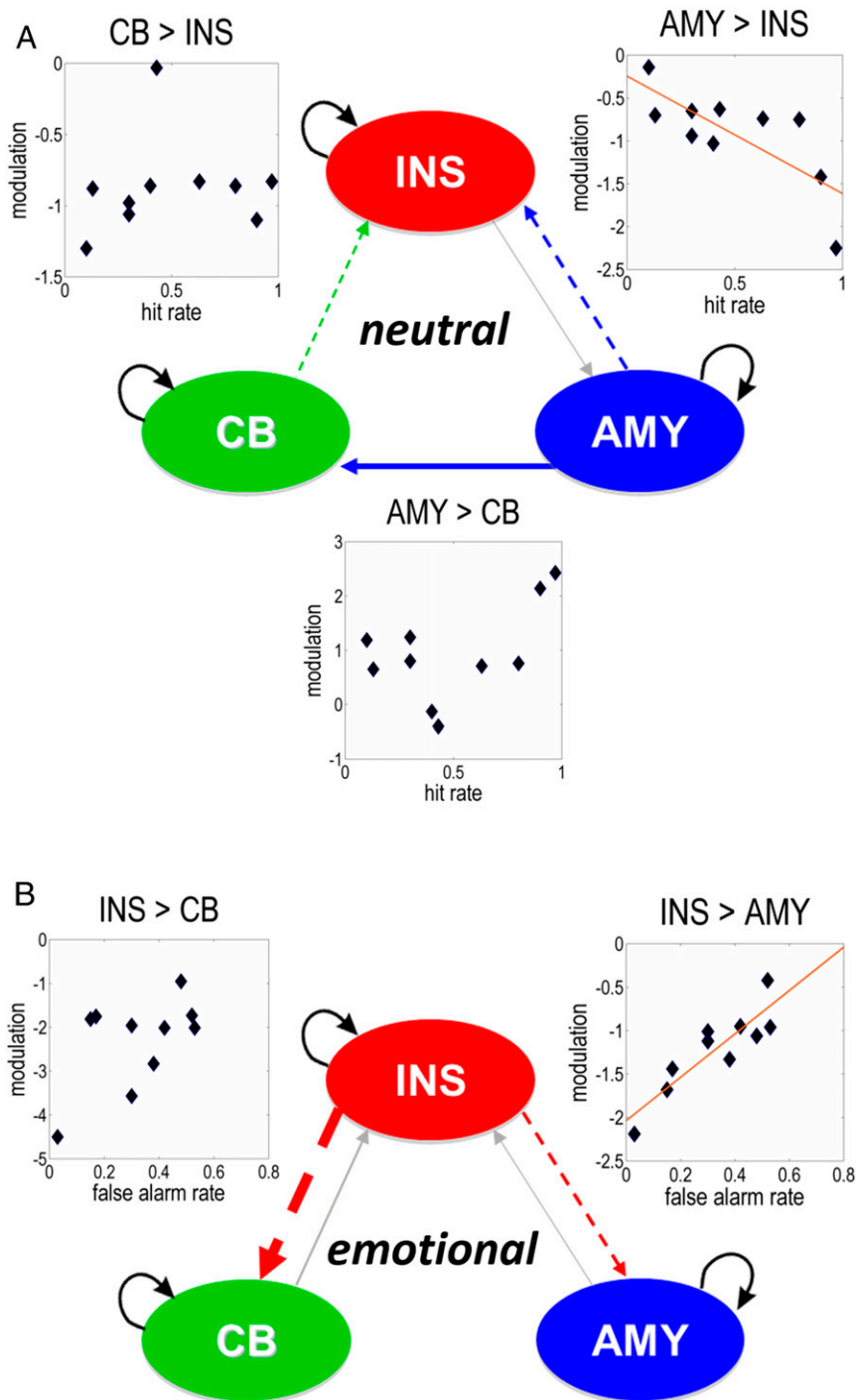


Fig. 2. Effective connectivity and its relationship to the perception of neutral body language. (A) Processing of neutral knocking led to negative (i.e., inhibitory; dashed arrows) effective connectivity from the amygdala (AMY) and cerebellar uvula (CB) to the insula (INS) and to positive (excitatory; solid arrows) effective connectivity from the AMY to CB. The hit rate for neutral knocking correlated inversely with changes in connectivity from the AMY to INS (Pearson correlation, $r = -0.75$, $P = 0.01$). There was no significant correlation between hit rate and changes in connectivity from the AMY to CB ($r = 0.51$, n.s.) or from the CB to INS (Spearman's rho, $r_s = 0.49$, n.s.). (B) During the processing of emotional knocking, the INS exhibited negative effective connectivity to the CB and AMY. Changes in effective connectivity from the INS to AMY were correlated positively with the false alarm rate ($r = 0.88$, $P < 0.001$). No significant correlation was found between changes in effective connectivity from the INS to CB and false alarm rate ($r = 0.55$, n.s.). Arrow width corresponds to the strength of effective connections. Solid arrows represent excitatory and dashed arrows stand for inhibitory effective connectivity. Gray arrows depict baseline connectivity, while colored arrows refer to the combined effects of baseline connectivity and its condition-specific modulation. Modulation refers to changes in connectivity induced by neutral or emotional processing (in Hertz). Black arrow loops represent self-connections of the regions.

functional diversity within the amygdala. Intrinsic interactions between functionally heterogeneous amygdala nuclei and their cross-talk with the insula may thus contribute to the control of emotional processing.

The cerebellar vermis has been hypothesized to communicate with the limbic system (27). The present analysis disclosed specific cerebellar afference from the amygdala during the processing of neutral body motion and from the insula during observation of emotional body language. This afference along with the absence of correlations between cerebellar effective connectivity and performance suggested that the vermis may not be primarily concerned with the processing of emotional stimuli. Instead, in agreement with brain stimulation (28) and clinical observations in the cerebellar cognitive affective syndrome (29), the cerebellar vermis may contribute to affect regulation. The cerebellum is increasingly considered to adapt internal models in similar ways across different functional domains. This is accomplished through reciprocal connections with subcortical and cortical supratentorial structures (30–33). By analogy with recent work on sensorimotor computations related to self-motion (34), the cerebellar uvula may use the information about the emotional valence of stimuli processed by the amygdala and insula toward adapting and thus, regulating mood.

Patients with neuropsychiatric conditions such as depression and schizophrenia tend to misinterpret neutral signals as emotional (35, 36). The neural correlates of this phenomenon remain largely unknown, as functional brain imaging in patients and healthy individuals alike has focused on contrasting emotional with neutral stimuli. Recent data point to aberrant resting-state functional connectivity between the insula and amygdala in patients with depression (37). Alterations in functional and structural connectivity between the insula and amygdala have also been related to anxiety levels in typically developing individuals (38). Assessing patients using the present methodology could help to understand how the insula, amygdala, and cerebellar vermis are involved in dysregulated emotional perception and mood. Associations between behavior and aberrations in this subcortical circuitry may also extend the spectrum of neuroimaging-based biomarkers for neuropsychiatric conditions (39).

Inferring the absence of emotional content from body language not only varies with presence of neuropsychiatric disorder but also, depends on gender. Already in nonhuman primates, females are better tuned to body motion than males (40). Women also surpass males in the recognition of neutral point-light knocking (41). Irrespective of observer's gender, happy female but angry male walking with subtle emotional expression is most often mistaken for neutral locomotion (42). The neurobiological mechanisms underlying such gender differences remain to be clarified, including potential differences in gray matter volume (43) and effective and anatomical white matter connectivity (6, 44–46). Furthermore, it appears of interest to assess the overall and gender-specific effects of extreme social distancing and isolation (such as during the COVID-19 pandemic) on body language reading and the corresponding brain circuits as well as associated measures of social cognition, behavior, and empathy.

In conclusion, the interplay between the amygdala and insula contributes substantially to the processing of social signals that convey emotionally neutral information, underwriting a fundamental yet underestimated component of adaptive social cognition and behavior. In light of previous research and theoretical models, the present findings identify the functional architecture of this network. Particular nuclei of the amygdala could be tuned to stimuli lacking emotional content, the cerebellar vermis could use external inputs to adapt internal affect, and the insula could serve as an integrator and moderator that silences the other two components during the evaluation of affective bodily signals. Further efforts are required to clarify whether this network may

also underwrite the recognition of emotionally neutral content in social signals beyond body language. Future research will contribute to differentiating the heterogeneous intrinsic circuits of the amygdala as well as their interaction with the insula, cerebellar vermis, and cortical networks for emotional inference and regulation.

Methods

Participants. We studied 17 right-handed male participants (age 27.9 ± 5.95 years, mean \pm SD) with normal vision and without history of neurological and psychiatric conditions or drug use. The recruitment of participants of the same gender ensured a homogenous group and thus, avoided potential confounds. Hemodynamic response in females has been shown to depend on menstrual cycle (47). Furthermore, gender appears to affect both neuromagnetic and hemodynamic correlates of body motion processing (48, 49). The group of participants overlapped with those analyzed in previous research (6, 46, 50, 51). Participants were enrolled following informed written consent and received financial reimbursement for partaking in the study. This research was approved by the local ethics committee of the University of Tübingen Medical School.

Knocking Displays. The stimuli were point-light animations of otherwise invisible female and male actors facing right and knocking on a door with neutral or emotional (happy and angry) expressions (Fig. 1A and Movie S1). The animations were created by three-dimensional (3D) recording (Optotrak; Northern Digital Inc.) of the movement of the head, right shoulder, elbow, wrist, and first and fourth metacarpal joints (52). Stimulus duration was 1,000 ms. A total of 90 trials consisting of emotional and neutral stimuli were presented. The order of stimuli was pseudorandomized, and stimulus onset intervals were jittered between 4,000 and 8,000 ms in steps of 500 ms, in order to optimize the estimation of hemodynamic responses. In an event-related design, the participants were presented with five task periods (18 trials per expression) of 108 s each and six baseline epochs of 24 s each, resulting in a total session duration of 684 s. The stimuli were projected onto a screen outside the MRI scanner. They were viewed by the participants through a tilted mirror on the head coil, subtending a visual angle of $\sim 3^\circ$ in height and 2° in width. On each trial, participants indicated the emotion they perceived by pressing the corresponding button (button assignment was counterbalanced between participants).

MRI Acquisition. The imaging data were acquired on a 3T MRI scanner (TimTrio; Siemens Medical Solutions; 12-channel head coil). A 3D magnetization-prepared rapid gradient echo dataset (176 sagittal slices, repetition time (TR) = 2,300 ms, echo time (TE) = 2.92 ms, inversion time (TI) = 1,100 ms, voxel size = $1 \times 1 \times 1 \text{ mm}^3$) was obtained, followed by a field map for inhomogeneity correction. Functional echo-planar imaging (EPI; 171 volumes, 56 axial slices, TR = 4,000 ms, TE = 35 ms, in-plane resolution: $2 \times 2 \text{ mm}^2$, slice thickness = 2 mm, 1-mm gap) was recorded during performance of the task.

MRI Data Processing and Analysis. Preprocessing of fMRI data followed standard procedures implemented in the Statistical Parametric Mapping (SPM) software (SPM12, Wellcome Centre for Human Neuroimaging, Institute of Neurology, University College London; <https://www.fil.ion.ucl.ac.uk/spm>). This involved slice timing correction, realignment, unwarping, image coregistration, segmentation-based normalization, and smoothing. In the exploratory fMRI whole-brain analysis, a general linear model (GLM) was specified for the EPI data, with the first and second regressors of interest encoding the onsets of neutral and emotional (happy and angry) stimuli, respectively. Regressors of no interest were included for trials with missing responses, six head motion parameters, and time series from white matter and cerebrospinal fluid. A high-pass filter (cutoff frequency 1/256 Hz) was implemented, and a first-order autoregressive process (coefficient of 0.2) was used to account for serial autocorrelations. Subject-specific contrast images testing for neutral vs. emotional effects were submitted to second-level (between-subject) random effects analyses. Second-level activations (FWE corrected for multiple comparisons at a $P < 0.05$ voxel-wise threshold) were attributed to brain regions using automated anatomical labeling in SPM (53) and the [NeuroSynth.org](https://neurosynth.org) database (<https://neurosynth.org>) (54).

DCM. The three regions showing significant responses to neutral and emotional point-light knocking were included in a DCM analysis. The first eigenvariate of all activated voxels ($P < 0.05$, uncorrected) within 8 mm of the

individual regional maximum was used to summarize regional responses. Subsequently, one-state, bilinear, deterministic DCMs with reciprocal extrinsic (between-region) connections between all nodes were created for every participant. Both regressors of interest from the GLM were specified as driving input reaching all nodes included in the DCM: the amygdala, insula, and cerebellar vermis. Based on the results of the SPM analysis, the first GLM regressor of interest (neutral body language) was used to modulate all connections from the amygdala and cerebellar vermis. Emotional body language (the second GLM regressor of interest) was specified to modulate all connections from the insula. These full models of effective connectivity were fitted to each participant's fMRI data, yielding the so-called posterior connectivity parameters and their probabilities.

Parametric Empirical Bayes. The posterior connectivity parameter estimates from all participants' DCMs were assessed at the group level using parametric empirical Bayes (PEB) and BMR (7). The PEB framework affords robust group-level analyses of effective connectivity by means of a hierarchical model, comprising DCMs at the single-subject level and a GLM of connectivity parameters at the between-subject level. After estimating the PEB model, parameters that did not contribute to the model evidence were pruned using BMR. This entailed a rapid automatic search over the space of connectivity parameters, which identified a minimal set needed to explain the data. A preliminary BMR analysis indicated that the most probable models were those with driving input to the amygdala and insula (posterior parameter probabilities of 96 and 98%, respectively). The full PEB model for the main BMR analysis thus only included driving input on these two nodes. The posterior parameter estimates following BMR were averaged using Bayesian model averaging (BMA), and the ensuing BMA parameters (with a posterior probability at or above 95%) are reported in

SI Appendix, Table S1. The resulting pattern of effective connectivity is illustrated in Fig. 2.

Behavior Analyses. For each participant, hit and false alarm rates for neutral stimuli were calculated. We extracted the individual modulatory DCM parameters (with a posterior probability at or above 95 % after BMA) for the participants with an accuracy (hit rate to neutral knocking) below 1.0. The behavioral and connectivity parameters were submitted to correlation analyses, corrected for multiple comparisons. All behavioral and connectivity data were tested for normality of distribution by Shapiro–Wilk tests with subsequent uses of either parametric (Pearson product–moment correlation) or nonparametric (Spearman correlation) statistics.

Data Availability. The code for the effective connectivity analyses is available within the SPM12 software package (<https://www.fil.ion.ucl.ac.uk/spm>). All relevant data are included in the manuscript and *SI Appendix*.

ACKNOWLEDGMENTS. We thank Alexander N. Sokolov, Richard S. J. Frackowiak, and Patrik Vuilleumier for valuable discussion. Technical support was provided by Ric Davis, Jürgen Dax, Chris Freemantle, Bernd Kardatzki, Rachael Maddock, and Liam Reilly, and administrative assistance by Marcia Bennett, David Blundred, Kamlyn Ramkissoon, Tracy Skinner, and Daniela Warr. This research was supported by fellowships from the Leenaards Foundation (to A.A.S.), the Baasch-Medicus Foundation (to A.A.S.), the Swiss National Science Foundation (to A.A.S.), and the European Academy of Neurology (to A.A.S.); grants from the Helmut Horten Foundation (to A.A.S.) and the Synapsis Foundation - Alzheimer Research Switzerland ARS (to A.A.S.); Wellcome Trust Principal Research Fellowship 088130/Z/09/Z (to K.J.F.); grants from the Reinhold Beilich Foundation (to M.A.P.) and the BBBank Foundation (to M.A.P.); and German Research Foundation Grant DFG PA 847/22-1 (to M.A.P.).

1. M. Tamietto, B. de Gelder, Neural bases of the non-conscious perception of emotional signals. *Nat. Rev. Neurosci.* **11**, 697–709 (2010).
2. M. A. Pavlova, Biological motion processing as a hallmark of social cognition. *Cereb. Cortex* **22**, 981–995 (2012).
3. S. K. Brooks *et al.*, The psychological impact of quarantine and how to reduce it: Rapid review of the evidence. *Lancet* **395**, 912–920 (2020).
4. S. Li, Y. Wang, J. Xue, N. Zhao, T. Zhu, The impact of COVID-19 epidemic declaration on psychological consequences: A study on active Weibo users. *Int. J. Environ. Res. Public Health* **17**, E2032 (2020).
5. H. H. Thorp, Time to pull together. *Science* **367**, 1282 (2020).
6. A. A. Sokolov *et al.*, Structural and effective brain connectivity underlying biological motion detection. *Proc. Natl. Acad. Sci. U.S.A.* **115**, E12034–E12042 (2018).
7. K. J. Friston *et al.*, Bayesian model reduction and empirical Bayes for group (DCM) studies. *Neuroimage* **128**, 413–431 (2016).
8. M. M. Mesulam, E. J. Mufson, Insula of the old world monkey. III. Efferent cortical output and comments on function. *J. Comp. Neurol.* **212**, 38–52 (1982).
9. F. Kurth, K. Zilles, P. T. Fox, A. R. Laird, S. B. Eickhoff, A link between the systems: Functional differentiation and integration within the human insula revealed by meta-analysis. *Brain Struct. Funct.* **214**, 519–534 (2010).
10. L. Pessoa, R. Adolphs, Emotion processing and the amygdala: From a “low road” to “many roads” of evaluating biological significance. *Nat. Rev. Neurosci.* **11**, 773–783 (2010).
11. R. Adolphs, D. Tranel, H. Damasio, A. Damasio, Impaired recognition of emotion in facial expressions following bilateral damage to the human amygdala. *Nature* **372**, 669–672 (1994).
12. H. C. Breiter *et al.*, Response and habituation of the human amygdala during visual processing of facial expression. *Neuron* **17**, 875–887 (1996).
13. J. S. Morris *et al.*, A differential neural response in the human amygdala to fearful and happy facial expressions. *Nature* **383**, 812–815 (1996).
14. P. Vuilleumier, J. L. Armony, J. Driver, R. J. Dolan, Effects of attention and emotion on face processing in the human brain: An event-related fMRI study. *Neuron* **30**, 829–841 (2001).
15. R. Adolphs, Fear, faces, and the human amygdala. *Curr. Opin. Neurobiol.* **18**, 166–172 (2008).
16. L. Pessoa, Emotion and cognition and the amygdala: From “what is it?” to “what’s to be done?”. *Neuropsychologia* **48**, 3416–3429 (2010).
17. A. Bechara, H. Damasio, A. R. Damasio, Role of the amygdala in decision-making. *Ann. N. Y. Acad. Sci.* **985**, 356–369 (2003).
18. S. W. Chang *et al.*, Neural mechanisms of social decision-making in the primate amygdala. *Proc. Natl. Acad. Sci. U.S.A.* **112**, 16012–16017 (2015).
19. A. Amir, S. C. Lee, D. B. Headley, M. M. Herzallah, D. Pare, Amygdala signaling during foraging in a hazardous environment. *J. Neurosci.* **35**, 12994–13005 (2015).
20. V. D. Costa, A. R. Mitz, B. B. Averbach, Subcortical substrates of explore-exploit decisions in primates. *Neuron* **103**, 533–545.e5 (2019).
21. G. Pourtois *et al.*, Errors recruit both cognitive and emotional monitoring systems: Simultaneous intracranial recordings in the dorsal anterior cingulate gyrus and amygdala combined with fMRI. *Neuropsychologia* **48**, 1144–1159 (2010).
22. R. Guex *et al.*, Neurophysiological evidence for early modulation of amygdala activity by emotional reappraisal. *Biol. Psychol.* **145**, 211–223 (2019).
23. D. Bzdok, A. R. Laird, K. Zilles, P. T. Fox, S. B. Eickhoff, An investigation of the structural, connective, and functional subspecialization in the human amygdala. *Hum. Brain Mapp.* **34**, 3247–3266 (2013).
24. M. Gamer, B. Zurovski, C. Büchel, Different amygdala subregions mediate valence-related and attentional effects of oxytocin in humans. *Proc. Natl. Acad. Sci. U.S.A.* **107**, 9400–9405 (2010).
25. I. Ehrlich *et al.*, Amygdala inhibitory circuits and the control of fear memory. *Neuron* **62**, 757–771 (2009).
26. U. Mayer, O. Rosa-Salva, J. L. Loveland, G. Vallortigara, Selective response of the nucleus taeniae of the amygdala to a naturalistic social stimulus in visually naive domestic chicks. *Sci. Rep.* **9**, 9849 (2019).
27. J. D. Schmahmann, J. B. Weilburg, J. C. Sherman, The neuropsychiatry of the cerebellum—insights from the clinic. *Cerebellum* **6**, 254–267 (2007).
28. D. J. Schutter, J. van Honk, The cerebellum in emotion regulation: A repetitive transcranial magnetic stimulation study. *Cerebellum* **8**, 28–34 (2009).
29. J. D. Schmahmann, J. C. Sherman, The cerebellar cognitive affective syndrome. *Brain* **121**, 561–579 (1998).
30. P. L. Strick, R. P. Dum, J. A. Fiez, Cerebellum and nonmotor function. *Annu. Rev. Neurosci.* **32**, 413–434 (2009).
31. A. A. Sokolov, R. C. Miall, R. B. Ivry, The cerebellum: Adaptive prediction for movement and cognition. *Trends Cogn. Sci. (Regul. Ed.)* **21**, 313–332 (2017).
32. A. C. Bostan, P. L. Strick, The basal ganglia and the cerebellum: Nodes in an integrated network. *Nat. Rev. Neurosci.* **19**, 338–350 (2018).
33. A. A. Sokolov, The cerebellum in social cognition. *Front. Cell. Neurosci.* **12**, 145 (2018).
34. J. X. Brooks, J. Carriot, K. E. Cullen, Learning to expect the unexpected: Rapid updating in primate cerebellum during voluntary self-motion. *Nat. Neurosci.* **18**, 1310–1317 (2015).
35. J. M. Leppänen, M. Milders, J. S. Bell, E. Terriere, J. K. Hietanen, Depression biases the recognition of emotionally neutral faces. *Psychiatry Res.* **128**, 123–133 (2004).
36. S. Potvin, A. Tikász, A. Mendrek, Emotionally neutral stimuli are not neutral in schizophrenia: A mini review of functional neuroimaging studies. *Front. Psychiatry* **7**, 115 (2016).
37. R. Ramasubbu *et al.*, Reduced intrinsic connectivity of amygdala in adults with major depressive disorder. *Front. Psychiatry* **5**, 17 (2014).
38. V. Baur, J. Hänggi, N. Langer, L. Jäncke, Resting-state functional and structural connectivity within an insula-amygdala route specifically index state and trait anxiety. *Biol. Psychiatry* **73**, 85–92 (2013).
39. M. D. Kaiser *et al.*, Neural signatures of autism. *Proc. Natl. Acad. Sci. U.S.A.* **107**, 21223–21228 (2010).
40. J. Brown, G. Kaplan, L. J. Rogers, G. Vallortigara, Perception of biological motion in common marmosets (*Callithrix jacchus*): By females only. *Anim. Cogn.* **13**, 555–564 (2010).
41. A. A. Sokolov, S. Krüger, P. Enck, I. Krägeloh-Mann, M. A. Pavlova, Gender affects body language reading. *Front. Psychol.* **2**, 16 (2011).
42. S. Krüger, A. N. Sokolov, P. Enck, I. Krägeloh-Mann, M. A. Pavlova, Emotion through locomotion: Gender impact. *PLoS One* **8**, e81716 (2013).

43. D. Stam, Y. A. Huang, J. Van den Stock, Non-overlapping and inverse associations between the sexes in structural brain-trait associations. *Front. Psychol.* **10**, 904 (2019).
44. M. A. Pavlova, Sex and gender affect the social brain: Beyond simplicity. *J. Neurosci. Res.* **95**, 235–250 (2017).
45. M. Ingalhalikar *et al.*, Sex differences in the structural connectome of the human brain. *Proc. Natl. Acad. Sci. U.S.A.* **111**, 823–828 (2014).
46. A. A. Sokolov *et al.*, Linking structural and effective brain connectivity: Structurally informed parametric empirical Bayes (si-PEB). *Brain Struct. Funct.* **224**, 205–217 (2019).
47. J. M. Goldstein, M. Jerram, B. Abbs, S. Whitfield-Gabrieli, N. Makris, Sex differences in stress response circuitry activation dependent on female hormonal cycle. *J. Neurosci.* **30**, 431–438 (2010).
48. L. C. Anderson *et al.*, Sex differences in the development of brain mechanisms for processing biological motion. *Neuroimage* **83**, 751–760 (2013).
49. M. A. Pavlova, A. N. Sokolov, C. Bidet-Iledei, Sex differences in the neuromagnetic cortical response to biological motion. *Cereb. Cortex* **25**, 3468–3474 (2015).
50. A. A. Sokolov *et al.*, Biological motion processing: The left cerebellum communicates with the right superior temporal sulcus. *Neuroimage* **59**, 2824–2830 (2012).
51. A. A. Sokolov, M. Erb, W. Grodd, M. A. Pavlova, Structural loop between the cerebellum and the superior temporal sulcus: Evidence from diffusion tensor imaging. *Cereb. Cortex* **24**, 626–632 (2014).
52. F. E. Pollick, H. M. Paterson, A. Bruderlin, A. J. Sanford, Perceiving affect from arm movement. *Cognition* **82**, B51–B61 (2001).
53. N. Tzourio-Mazoyer *et al.*, Automated anatomical labeling of activations in SPM using a macroscopic anatomical parcellation of the MNI MRI single-subject brain. *Neuroimage* **15**, 273–289 (2002).
54. T. Yarkoni, R. A. Poldrack, T. E. Nichols, D. C. Van Essen, T. D. Wager, Large-scale automated synthesis of human functional neuroimaging data. *Nat. Methods* **8**, 665–670 (2011).